Performance Analysis of Joint Multi-Antenna Spoofing Detection and Attitude Estimation

Andriy Konovaltsev, Manuel Cuntz, Christian Haettich, Michael Meurer
Institute of Communications and Navigation, German Aerospace Center (DLR)
Oberpfaffenhofen, Germany

BIOGRAPHY

Andriy Konovaltsev received his engineer diploma and the Ph.D. degree in electrical engineering from Kharkov State Technical University of Radio Electronics, Ukraine in 1993 and 1996, correspondingly. He joined the Institute of Communications and Navigation of DLR in 2001. His main research interest is in application of antenna array signal processing for improving performance of satellite navigation systems in challenging signal environments.

Manuel Cuntz received the diploma in electrical engineering degree in 2005 from the Technical University of Kaiserslautern. He joined the Institute of Communications and Navigation of DLR in June 2006. His fields of research are multi-antenna satellite navigation receivers.

Christian Haettich received his Master of Science in Embedded Systems in 2011 from HS Pforzheim University. Since March 2011, he is working at the Institute of Communications and Navigation of DLR. His current research interests are multi-antenna receivers and robust navigation signal processing.

Michael Meurer received the diploma in electrical engineering and the Ph.D. degree from the University of Kaiserslautern, Germany. After graduation, he joined the Research Group for Radio Communications at the Technical University of Kaiserslautern, Germany, as a senior key researcher, where he was involved in various international and national projects in the field of communications and navigation both as project coordinator and as technical contributor. From 2003 till 2005, Dr. Meurer was active as a senior lecturer. Since 2005 he has been an Associate Professor (PD) at the same university. Additionally, since 2006 Dr. Meurer is with the German Aerospace Centre (DLR), Institute of Communications and Navigation, where he is the director of the Department of Navigation and of the center of excellence for satellite navigation.

ABSTRACT

The paper presents the results of field tests of a technique for detection of spoofing signals using the direction-of-arrival (DOA) measurements obtained by processing signals of an adaptive antenna array. The detection of spoofing signals is achieved by comparing and statistical testing of the measured DOAs against the DOAs predicted with the ephemeris data. Because the attitude of the antenna array is assumed to be unknown and has to be estimated, the detection of spoofing signals is treated as a joint detection/estimation problem. For performing the field tests, a simple version of spoofing, so called meaconing, has been realized using a repeater of the in-air GNSS signals. The performance of the proposed technique has been investigated for both static and dynamic user cases.

INTRODUCTION

For those applications of global satellite navigation systems (GNSSs) which rely on the open-service navigation signals the reliable detection of spoofing attacks is of great importance. This is especially true for the applications with safety- and security-critical content. A great deal of research has been performed on finding solutions to the problem of GNSS spoofing, see for instance [1], [2] and references herein. Among the receiver-autonomous techniques for spoofing detection, the approach based on the use of spatial angles of arrival is considered to be the most powerful [3] as it enables to detect even the most sophisticated spoofing techniques realizable in practice.

The use of the spoofing detection based on spatial angle of arrival comes at price of more complex hardware because it requires multiple receiving antennas and RF front-ends as well as high computational power in digital signal processing. However the implementation of this approach in a GNSS receiver utilizing the technology of adaptive antenna arrays for radio interference mitigation is relatively simple and might only require a modification of the receiver baseband signal processing software. The array signal processing in such a receiver is used to control the array reception pattern with the help of adaptive beamforming and nulling. The estimation of the directions of arrival (DOAs) of incoming signals can be

used to constrain the adaptive beamforming and nulling processes, for example to maintain a constant gain and phase responses of the array system in the direction of a GNSS satellite. For this purpose the DOA estimation was also implemented in the demonstrator of a GNSS receiver with an adaptive antenna, GALANT [4], that is being developed by the Institute of Communications and Navigation of DLR. Recently, a technique [5] based on the use of the estimated directions of arrival of GNSS signals for a joint detection of spoofing and estimation of the array attitude has been proposed by the group of authors from the GALANT development team.

The advantages of using an array processing technique for direction finding for purposes of spoofing detection can be summarized as follows:

- this approach is fully complemental and can be easily used in combination with other spoofing detection techniques;
- directional information about spoofing signals can be used to mitigate them by generating spatial null(s) in the array reception pattern (see for example [6]);
- a network of GNSS receivers with antenna arrays performing the DOA estimation and detecting spoofing signals can enable the localization of spoofing transmitters.

Additionally, as discussed in [3], the multi-antenna techniques for spoofing detection can be only fooled by several phase-synchronous spoofing transmitters placed around the victim receiver. In order to produce consistent DOA estimations, the spoofing signals must be phase-aligned in such a way that the carrier phases of their sums at each array element correspond to the phases of the authentic signals. The required number of the synchronous transmitters is defined by the number of array elements which is usually equal or greater than four. As it can be seen, this scenario quickly becomes unfeasible in practice as it would require multiple precisely synchronized transmitters, exact knowledge about the coordinates of the array elements and about the characteristics of the propagation channel between the transmitters and the antenna array.

In the current paper we present results of field tests of the technique developed in [5]. A simple version of spoofing, so called meaconing or rebroadcast, was used in these tests. Apart from simple realization, the investigation of this type of spoofing has also practical interest since such interference is hard to handle with alternative approaches while it can also occur unintentionally. For example, improper installed repeaters aimed to improve indoor availability of GPS can act as meaconing sources [7].

The paper is organized as follows. The next section gives a short overview of the technique under test for joint spoofing detection and antenna attitude estimation that was proposed in [5]. Further in the next section, the results for a static user in interference-free signal conditions are presented. Results for static and dynamic users under meaconing signal conditions are discussed in the next two sections, correspondingly. The summary of the results and conclusions are given in the last section.

TECHNIQUE UNDER TEST

In order to discriminate between the spoofing and authentic GNSS signals, the technique proposed by the authors in [5] makes use of the direction of arrival information collected for all received signals. One part of this information comes from the positioning module of the receiver that, among others, calculates azimuth Az and elevation El angles of each visible GNSS satellite as viewed from the estimated user position. These angles are given in the local user's east-north-up (ENU) coordinate frame. The second part of the spatial information is obtained through estimation of the actual directions of arrival (φ, θ) of each satellite signal with the help of one of array signal processing methods for direction finding [8]. In this case, the estimated directions are referenced to the local antenna coordinate frame.

Under conditions without spoofing and meaconing, the DOAs predicted while performing the positioning solution and the ones estimated in the antenna array processing should be consistent with each other. The relationship between the N_{DOA} DOAs in these two sets can be mathematically formulated as follows:

$$\mathbf{D}_{loc} = \mathbf{R}(r,p,y)\mathbf{D}_{enu} + \mathbf{N} \qquad (1)$$

where

- $\mathbf{D}_{loc}$ is a $[3 \times N_{\mathrm{DOA}}]$ matrix composed of N_{DOA} unit vectors of directional cosines describing the directions of arrival of satellite signals in the local coordinate frame of the antenna array. A single directional cosine vector is defined as
  $\widehat{\boldsymbol{d}}_{loc} = [\sin\theta\cos\varphi\,, \sin\theta\sin\varphi\,, \cos\theta]^{\mathrm{T}}$,
  where θ is the elevation angle and φ is the azimuth angle in the antenna local coordinate frame;
- $\mathbf{D}_{enu}$ is a $[3 \times N_{\mathrm{DOA}}]$ matrix composed of unit vectors of directional cosines corresponding to the DOAs of satellite signals in the user ENU coordinate frame. Each such vector is defined as follows
  $\widehat{\boldsymbol{d}}_{enu} = [\cos El \sin Az\,, \cos El \cos Az\,, \sin El]^{\mathrm{T}}$
  where El and Az are the elevation and azimuth angles, correspondingly, in the ENU coordinate frame;
- $\mathbf{R}(r,p,y)$ is a $[3 \times 3]$ unitary rotation matrix (see [9], p.441) describing to the attitude of the antenna array defined by three Eulers angles: roll r, pitch p and yaw y. These angles are referred to the user local ENU coordinate frame;
- $\mathbf{N}$ is a $[3 \times N_{\mathrm{DOA}}]$ matrix describing the measurement noise effect. Further for simplicity, we assume that the noise components follow Gaussian distributions with zero means and, in general case, different standard deviations $\sigma_1, \sigma_2, \ldots, \sigma_{N_{DOA}}$.

The antenna attitude is estimated by solving (1) for Euler angles (r, p, y) in the least squares sense:

$$(\hat{r}, \hat{p}, \hat{y}) = \underset{r,p,y}{\arg\min} \|\mathbf{R}(r,p,y)\mathbf{D}_{enu} - \mathbf{D}_{loc}\|^2 . \qquad (2)$$

The least squares problem (2) can be solved iteratively by linearizing the non-linear cost function around some initial set of roll, pitch and yaw angles (r_0, p_0, y_0) using the Taylor expansion of the first order. As shown in [5], the iterative formulation for the solution of (2) is given by

$$\begin{pmatrix} r_{n+1} \\ p_{n+1} \\ y_{n+1} \end{pmatrix} = \begin{pmatrix} r_n \\ p_n \\ y_n \end{pmatrix} - ([\boldsymbol{\nabla}\mathbf{g}^{\mathrm{T}}(r_n, p_n, y_n)\,]^{\mathrm{T}})^{-1}\mathbf{g}(r_n, p_n, y_n). \qquad (3)$$

where $\mathbf{g}(r,p,y)$ is a vector which components are the functions of the Euler angles:

$$\mathbf{g}(r,p,y) = \begin{bmatrix} \mathrm{g}_r(r,p,y) \\ \mathrm{g}_p(r,p,y) \\ \mathrm{g}_y(r,p,y) \end{bmatrix} = \begin{bmatrix} \mathrm{trace}\left(\dfrac{\partial \mathbf{R}(r,p,y)}{\partial r}\mathbf{D}_{enu}\mathbf{D}_{loc}^{\mathrm{T}}\right) \\ \mathrm{trace}\left(\dfrac{\partial \mathbf{R}(r,p,y)}{\partial p}\mathbf{D}_{enu}\mathbf{D}_{loc}^{\mathrm{T}}\right) \\ \mathrm{trace}\left(\dfrac{\partial \mathbf{R}(r,p,y)}{\partial y}\mathbf{D}_{enu}\mathbf{D}_{loc}^{\mathrm{T}}\right) \end{bmatrix}, \qquad (4)$$

and $\boldsymbol{\nabla}$ is a vector differential operator defined as

$$\boldsymbol{\nabla} = \left(\frac{\partial}{\partial r} \quad \frac{\partial}{\partial p} \quad \frac{\partial}{\partial y}\right)^{\mathrm{T}}, \qquad (5)$$

so that the gradient term $[\boldsymbol{\nabla}\mathbf{g}^{\mathrm{T}}(r,p,y)\,]^{\mathrm{T}}$ produces the following $[3 \times 3]$ matrix

$$[\boldsymbol{\nabla}\mathbf{g}^{\mathrm{T}}(r,p,y)\,]^{\mathrm{T}} = \begin{bmatrix} \dfrac{\partial \mathrm{g}_r(r,p,y)}{\partial r} & \dfrac{\partial \mathrm{g}_r(r,p,y)}{\partial p} & \dfrac{\partial \mathrm{g}_r(r,p,y)}{\partial y} \\ \dfrac{\partial \mathrm{g}_p(r,p,y)}{\partial r} & \dfrac{\partial \mathrm{g}_p(r,p,y)}{\partial p} & \dfrac{\partial \mathrm{g}_p(r,p,y)}{\partial y} \\ \dfrac{\partial \mathrm{g}_y(r,p,y)}{\partial r} & \dfrac{\partial \mathrm{g}_y(r,p,y)}{\partial p} & \dfrac{\partial \mathrm{g}_y(r,p,y)}{\partial y} \end{bmatrix}. \qquad (6)$$

The starting set of Euler angles (r_0, p_0, y_0) in (3) can be calculated using the elements of the least-squares estimation $\widehat{\mathbf{R}}$ of the rotation matrix [9]:

$$\widehat{\mathbf{R}} = \underset{\mathbf{R}}{\arg\min} \|\mathbf{R}\,\mathbf{D}_{enu} - \mathbf{D}_{loc}\|^2 , \qquad (7)$$

and

$$\begin{aligned} \tan r_0 &= -\frac{\hat{R}_{13}}{\hat{R}_{33}}, \\ \tan p_0 &= -\frac{\hat{R}_{23}}{\sqrt{\hat{R}_{21}^2 + \hat{R}_{22}^2}}, \\ \tan y_0 &= -\frac{\hat{R}_{21}}{\hat{R}_{22}}. \end{aligned} \qquad (8)$$

Please note that the formulation of (7) does not account for the side condition $\mathbf{R}(r,p,y)\mathbf{R}^{\mathrm{T}}(r,p,y) = \mathbf{I}$ that originates from the definition of a rotation matrix. The least squares problem formulated by (7) is known in the literature as the Wahba's problem. A computationally effective solution of the problem is available using the singular value decomposition (SVD) technique [10].

The quality of the solution for the antenna attitude can be assessed using the sum of squares of errors (SSE) test statistics similar to how it is used with receiver autonomous integrity monitoring (RAIM) techniques. The SSE metric is defined as follows

$$SSE = \mathrm{trace}\{[\mathbf{R}(r,p,y)\mathbf{D}_{enu} - \mathbf{D}_{loc}]^{\mathrm{T}} \cdot \mathbf{R}_N^{-1}[\mathbf{R}(r,p,y)\mathbf{D}_{enu} - \mathbf{D}_{loc}]\}, \qquad (9)$$

where the inverse of the covariance matrix of the measurement noise $\mathbf{R}_N^{-1}$ is used for normalizing individual residuals of the least squares solution. Further, we assume that the individual DOA measurement errors are Gaussian and not correlated with each other and the matrix $\mathbf{R}_N$ is a diagonal matrix consisting of the error variances, $\sigma_1^2, \sigma_2^2, \ldots, \sigma_{N_{DOA}}^2$.

If no systematic offsets observed between the measured and predicted DOAs of the GNSS signals, the SSE metric defined by (9) follows a central chi-squared distribution with $k = (2N_{\mathrm{DOA}} - 3)$ degrees of freedom. In another case, if all or some of the measured DOAs are biased with respects to predicted DOAs, the SSE metric follows a non-central chi-squared distribution with the same number of degrees of freedom as above but with some non-zero non-centrality parameter λ:

$$\begin{aligned} &\mathrm{H}_0(\text{no error}):\ SSE \sim \chi^2(k) \\ &\mathrm{H}_1(\text{error}):\quad SSE \sim \chi'^2(k,\lambda) \\ &k = (2N_{\mathrm{DOA}} - 3) \\ &\lambda = \sum_{n=1}^{N_{\mathrm{DOA}}} \left(\frac{\Delta_n}{\sigma_n}\right)^2 \end{aligned} \qquad (10)$$

where

Δ_n is the bias in the n-th DOA measurement, this bias is expressed as a spatial angle ψ_n between two direction cosines vectors of the measured DOA $\widehat{\boldsymbol{d}}_{loc,n}$ and the predicted "almanac" DOA $\widehat{\boldsymbol{d}}_{enu,n}$:

$$\Delta_n = \psi_n = \arccos\left(\widehat{\boldsymbol{d}}_{loc,n}^{\mathrm{T}}\widehat{\boldsymbol{d}}_{enu,n}\right), \qquad (11)$$

σ_n is the standard deviation of the n-th DOA measurement error given in units of the spatial angle ψ_n.

An example of probability density functions (pdfs) of the SSE test statistics for H_0 and H_1 hypothesis are shown in Figure 1. These numerical results were obtained by Monte Carlo simulations of DOA measurements for seven GNSS satellites. The standard deviation of the DOA measurement error was assumed to have the elevation dependence shown in Figure 2.

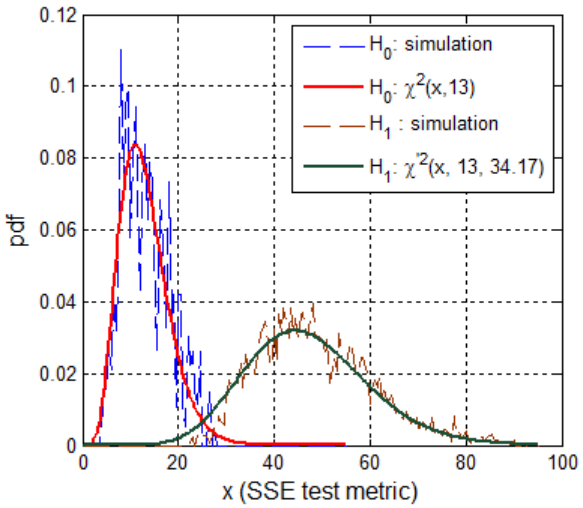

Figure 1: Pdfs of SSE test metric for H_0 and H_1 hypotheses

In simulations for the H_1 case, a single bias was introduced into the fifth DOA measurement: $\Delta_5 = 12.5°$ so that $(\Delta_5/\sigma_5)^2 = 34.17$.

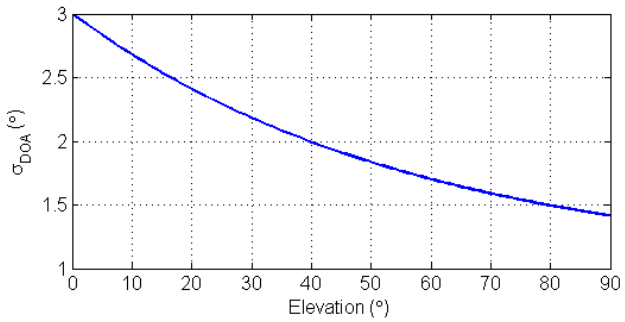

Figure 2: Approximation of dependency of DOA measurement error on satellite elevation in antenna local coordinate frame

As can be observed in Figure 1, the detection of the systematic biases in DOA measurements can be performed by using the Neyman-Pearson criterion, i.e. by setting a threshold for the SSE test metric defined by some desired false alarm rate. The presence of the systematic biases can then serve as one of indications of spoofer / meaconing attacks.

In practice, other sources of the DOA measurements biases have to be taken into account. The most common sources of such biases are the electromagnetic mutual coupling between the array elements and the multipath propagation. In order to evaluate the effects of these error sources on the false alarm performance of the proposed technique, the first tests were carried out in interference-free signal conditions. The results of these tests are presented in the next section.

FALSE ALARM PERFORMANCE

For investigating the false alarm performance of the technique for joint spoofing detection and attitude determination, the 2-by-2 rectangular adaptive antenna of the DLR GALANT receiver (see Figure 3, a) was mounted on the roof of the DLR Institute of Communications and Navigation in Oberpfaffenhofen (see Figure 3, b).

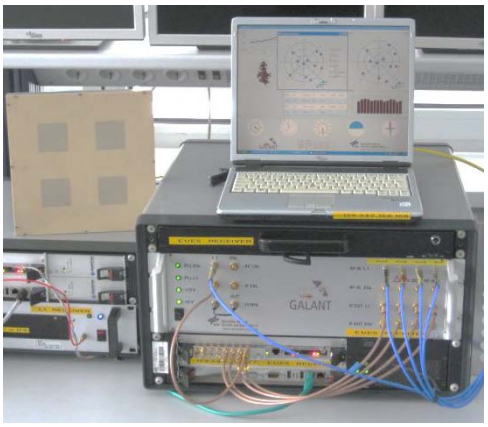

a)

b)

Figure 3: View of (a) GALANT multi-antenna receiver and (b) antenna array roof installation

Blocks of the array signal data were collected in each mutli-antenna satellite tracking channel and used in the

post-processing by a direction finding technique. In this study we used a unitary ESPRIT algorithm [11], [12] that is also used for the real-time DOA estimation in the receiver. The data blocks were collected simultaneously for up to 14 satellites signals being tracked by the receiver. Each array signal sample consists of complex-value outputs of four prompt PRN-code correlators. A single data block corresponds to the 50 ms of observation time and is of size $[4 \times 50]$.

The exemplary results for the estimated antenna attitude using two different non-overlapping sets of 1 hour of array signals data each are shown in Figure 4. The mean and standard deviations of the estimated Euler angles are given in Table 1.

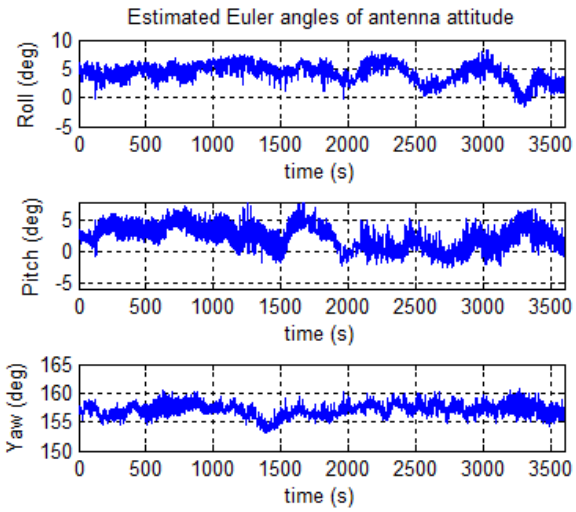

a) set #1

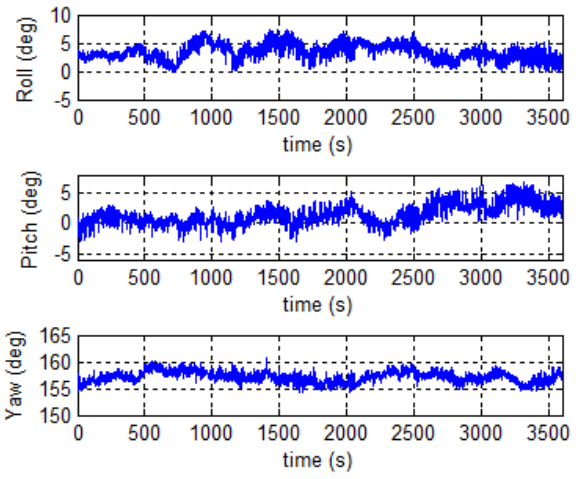

b) set #2

Figure 4: Estimated attitude of antenna array

It can be observed in Figure 4 that the estimated Euler angles may experience changes of up to 7-8 degrees over a time interval of several minutes. This is especially true for pitch and roll angles. The means and standard deviations estimated over 1 hour time window into two different data sets are consistent with each other.

	Yaw	*Pitch*	*Roll*
Mean (∘)	156.99	2.22	4.27
Std. (∘)	1.09	1.94	1.53

a) set #1

	Yaw	*Pitch*	*Roll*
Mean (∘)	157.14	1.40	3.48
Std. (∘)	1.00	1.66	1.41

b) set#2

Table 1: Mean and standard deviations of the attitude estimates performed on real DOA measurements

In order to account for DOA estimation biases due to the multipath and array mutual coupling effects, the entire set of DOA measurements was allowed to contain up to $N_{err,MAX}$ "natural" biases. The hypothesis H_1 is then assumed to be true if only any of the possible subsets with $N_{DOA} - N_{err,MAX}$ measurements delivers the SSE test metric above the detection threshold (see [5] for more details). In this study the value $N_{err,MAX} = 3$ was adopted. The accounting for the possible "naturally" biased DOA measurements results in the number of DOA measurements used for the attitude determination that changes with the time. This effect is illustrated by Figure 5. These results were obtained with the satellite elevation mask of 10°. As can be observed in Figure 5, the number of the actually used DOA measurements changes significantly and can fall down to 5 measurements even under open sky, interference-free conditions.

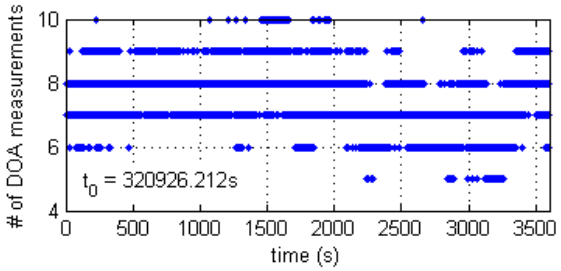

a) set #1

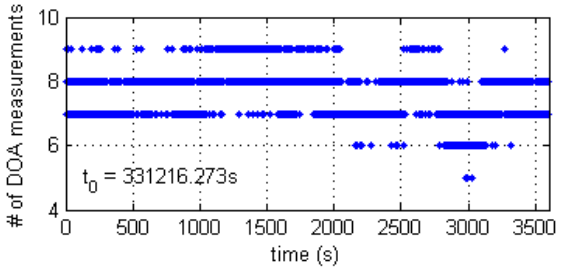

b) set #2

Figure 5: Number of estimated DOAs used for attitude determination

The next figure, Figure 6, presents the results for SSE test metric observed in the same two time windows as in Figure 4 and Figure 5. Please note that the detection threshold for the spoofing event in each time epoch depends on the number of used DOA measurements. The

results of testing the SSE statistics against the detection threshold are shown in Figure 6 as a status of the joint detection and estimation process. The status has three possible states: “valid”, “too few DOAs” and “spoofing”. Where “valid” means that no spoofing is detected and a valid solution for the antenna array attitude is obtained. The state “too few DOAs” indicates that no valid attitude solution is obtained and the number of DOA measurements available after the exclusion of biased measurements ($N_{err,MAX}$, at most) is too low, i.e. below 4. This state can be considered as the warning about a potential spoofing attack. The last, third possible state of the status flag is “spoofing” which is set if the SSE metric exceeds the spoofing detection threshold.

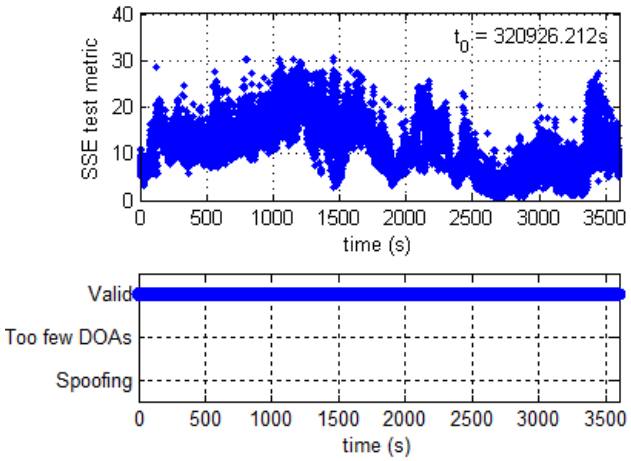

a) set #1

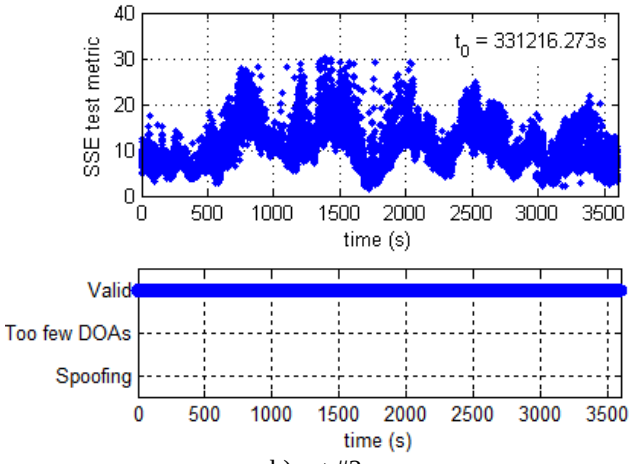

b) set #2

Figure 6: SSE test metric and status flags

As already discussed in [5], the DOA measurements delivered by the GALANT receiver show higher standard deviations of the DOA error as adopted in Figure 2. Therefore the elevation dependence of the DOA measurement error shown in Figure 2 was correspondingly scaled so that to avoid false alarm events in the interference free signal conditions. This adjustment resulted in $\sigma_{DOA}(El = 0°) = 6.9°$ and $\sigma_{DOA}(90°) = 3.3°$. These settings were also used by post-processing the collected array data in the field trials under the meaconing conditions described in the next two sections.

DETECTION PERFORMANCE, STATIC USER

The measurement set-up used with a static user scenario is shown in Figure 7. For simplicity, a re-transmitter of GNSS in-air signals was built up and served as the source of interfering signals simulating a meaconing attack.

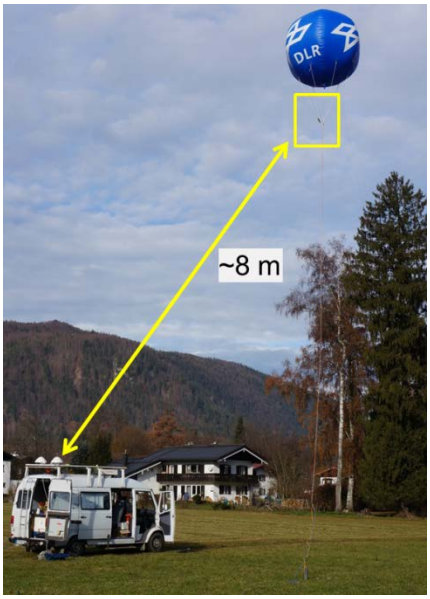

a) view of measurements location

b) zoomed view of transmitting antenna of repeater

c) antenna arrays of GALANT receiver installed on the roof of measurement van

Figure 7: Set-up used with static user tests

A balloon was used as the carrier of repeater transmitting antenna. The receiving antenna was installed about 50 m away from the balloon base in order to avoid the self-excitation through coupling between the repeater antennas. A low-noise amplifier was used to compensate for cabling losses in the re-transmitter signal chain. The

power of re-transmitted GNSS signals was adjusted with the help of a variable attenuation to such a minimum level where the satellite channels of the GALANT receiver still could be captured by the repeater signals without losing the lock on the signals in tracking.

The results obtained for SSE test metric, the status flags and the receiver estimated position are shown in Figure 8. It can be seen that the SSE metric (see Figure 8, a) changes by more than order of magnitude (please compare to Figure 6) when the repeater is switched on. Due to this, the time evolution of the status flag (see Figure 8, b) demonstrates a very clear transition from the "valid" to "spoofing" states. The effect of capturing the receiver tracking loops by the repeater signals can be also clearly observed in the estimated position (see Figure 8, c). It can be also observed that the detection of the presence of the repeater signals occurs simultaneously with the changes in the estimated position.

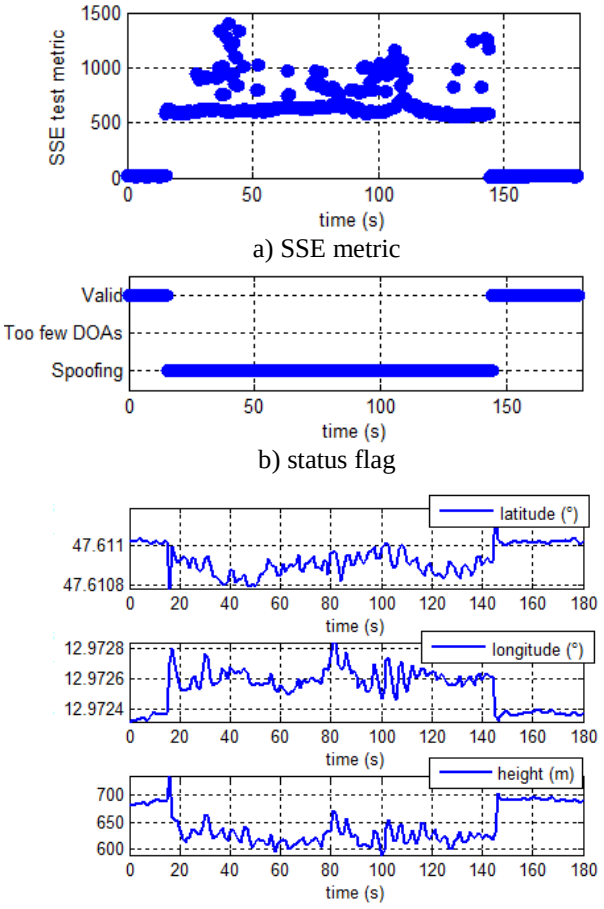

a) SSE metric

b) status flag

c) position estimation by receiver

Figure 8: Results of static user tests

The exemplary results for the estimated directions of arrival of the GPS navigation signals before and after activating the repeater are shown in Figure 9. In the latter case, all estimated DOAs are located around one point on the skyplot (see Figure 9, b), which explains the observed large jump of SSE metric values.

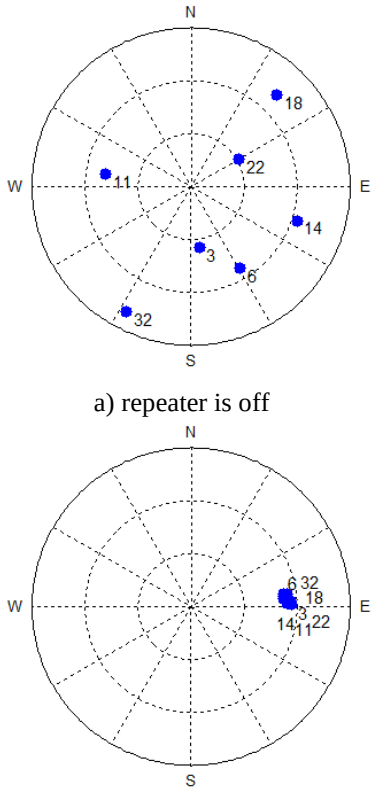

a) repeater is off

b) repeater is on

Figure 9: Examples of direction estimation results in repeater test for static user

DETECTION PERFORMANCE, DYNAMIC USER

In this test the balloon with the repeater transmitting antenna was fixed at the side of a rural road (see Figure 10). The measurement van was driving along the street with the speed of approximately 40 km/h making a roundtrip (see Figure 11) and passing two times by the installation place of the balloon.

The results obtained in the dynamic user scenario are shown in Figure 12 and Figure 13. Two time windows, each of approximately 50 s long, at which the effect of the repeater can be clearly seen, are marked in the figures with the help of half-transparent red blocks. It can be observed that the SSE test metric (see Figure 12,a) significantly grows in the time-windows with the repeater effect. This growth is especially large in the second window where the measurement van on the way back was on the road lane that is closer to the repeater installation (see Figure 10). The highest values of the SSE metric in both time windows are comparable to the corresponding values obtained in the static user scenario (see Figure 8, a). However, the time evolution of the status flag (see Figure 12, b) does not show such clear transitions between the "valid" and "spoofed" states as in Figure 8, b.

Figure 10: View of measurement location used with repeater test for dynamic user

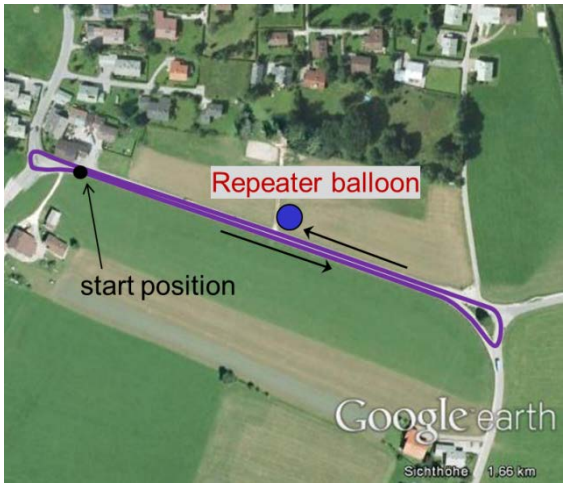

Figure 11: Route of measurements van in dynamic user test

The use of the simple re-transmitter as the spoofing source results in very unstable signal tracking while the tracking loops of the receiver are being captured by the repeater signals. This leads to often loss of locks and, because the direction finding is performed after the PRN code correlation, low number of DOA measurements available at a time. Please note that only satellites signals of GPS were used in these tests. The maximum number of the satellites in tracking at a time was not exceeding 8.

As can be observed in Figure 12,c the proposed joint spoofing detection and attitude determination technique is still able to at least warn the user about the meaconing attack before the estimated user position is significantly spoofed. It is also noticeable that the SSE test statistic can recover from the repeater effect faster than the estimated user position. This can be clearly observed in the second half of the first time-window where the consistent solutions for the antenna attitude are often available (see Figure 13) while the positioning solution is still erroneous or unavailable. This is due to the fact that the information required for the DOA estimation and antenna attitude determination is generated at lower signal processing level as compared to the position estimation. Also, the attitude determination is more robust against spoofing of single navigation signals due to the exclusion procedure of "naturally" biased DOA measurements described above.

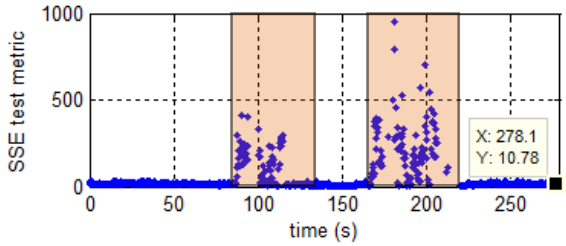

a) SSE metric

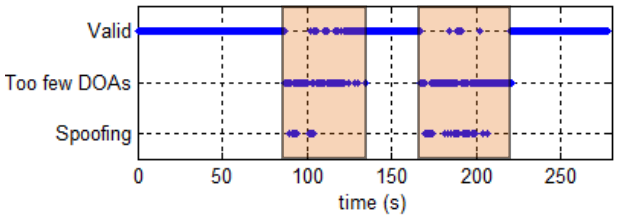

b) status flag

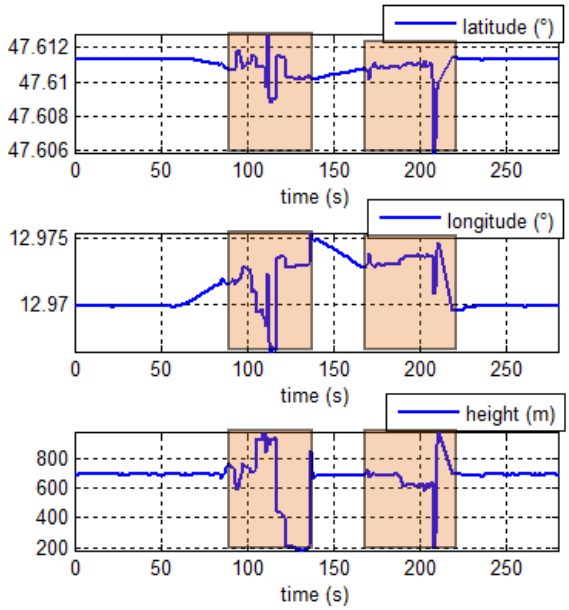

c) position estimation by receiver

Figure 12: Results of dynamic user tests

SUMMARY AND CONCLUSIONS

In this paper, field test results for a technique proposed for joint spoofing detection and antenna array attitude determination have been presented. The tests were carried out using DLR's proprietary multi-antenna receiver system. It has been shown that the tested technique is able to operate without false alarm events in interference-free

signal conditions. This was achieved by corresponding scaling of the weighting function describing the dependence of the DOA measurement error on the satellite elevation.

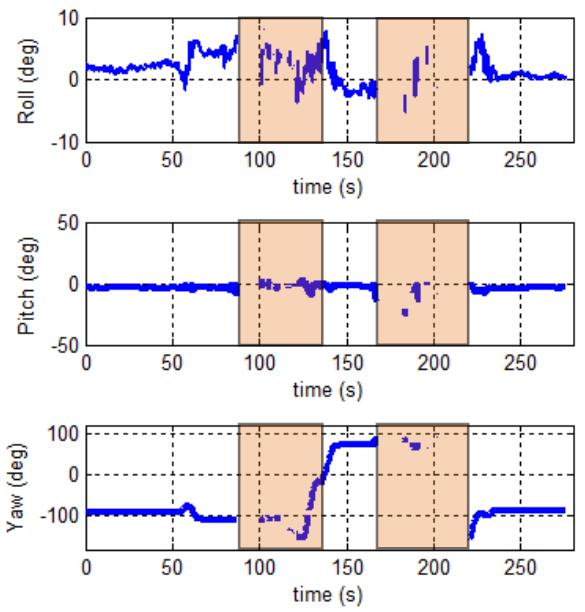

Figure 13: Results for antenna attitude in dynamic user tests

Under meaconing conditions the tested technique was able to detect the presence of the re-transmitted GNSS signals by making use of their estimated directions of arrival. A clear transition to the "spoofing" alarm state was observed in the static user scenario. In the scenario with the dynamic user, clear transitions to the "spoofing" alarm state were often hindered by low available number of DOA measurements resulted from unstable signal tracking and frequent losses of lock. However, low availability of the DOA measurements in combination with the frequent losses of lock in the receiver tracking channels can also serve as a good warning about the spoofing attack.

The following research topics can be addressed in the next studies:

(i) extension of the DOA estimation for considering more than one propagation path per satellite; this is especially interesting with respect to mitigation of spoofing, it can also help to handle the DOA estimation errors due to multipath effect;

(ii) use of the directional information about detected spoofing signals for their mitigation by generating spatial nulls in the reception pattern of the antenna array;

(iii) accounting for electromagnetic mutual coupling between the array elements in the DOA estimation;

(iv) considering the use of sequential attitude estimation.

ACKNOWLEDGMENTS

The research leading to the results reported in this paper has received funding from the European Community's Seventh Framework Programme (FP7/2007-2013) under grant agreement n°287207 as well as the funding through DLR Project Directorate for Space Research in the frame of DLR internal research and development project "Dependable Navigation". This support is greatly acknowledged.

REFERENCES

[1] T. E. Humphreys, B. Ledvina, and M. Psiaki, "Assessing the spoofing threat: Development of a portable GPS civilian spoofer," in *Proceedings of ION GNSS 2008*, 2008, p. 12.

[2] K. Wesson, D. Shepard, and T. Humphreys, "Straight Talk on Anti-Spoofing Securing the Future of PNT," *GPS World*, no. January, 2012.

[3] P. Montgomery and T. E. Humphreys, "A Multi-Antenna Defense: Receiver-Autonomous GPS Spoofing Detection," *Inside GNSS*, no. March/April, pp. 40–46, 2009.

[4] M. V. T. Heckler, M. Cuntz, A. Konovaltsev, L. A. Greda, A. Dreher, and M. Meurer, "Development of Robust Safety-of-Life Navigation Receivers," *IEEE Transactions on Microwave Theory and Techniques*, vol. 59, no. 4, pp. 998–1005, Apr. 2011.

[5] M. Meurer, A. Konovaltsev, M. Cuntz, and C. Hättich, "Robust Joint Multi-Antenna Spoofing Detection and Attitude Estimation using Direction Assisted Multiple Hypotheses RAIM," in *Proc. ION GNSS 2012*, 2012.

[6] C. E. McDowell, "GPS spoofer and repeater mitigation system using digital spatial nulling," U.S. Patent US 7250903 B1,2007.

[7] A. J. Van Dierendonck, "Treatment of re-radiated GNSS," in *Proceedings of Munich Satellite Navigation Summit*, 2009.

[8] H. L. V. Trees, *Optimum Array Processing (Detection, Estimation, and Modulation Theory, Part IV)*. Wiley-Interscience, 2002, p. 1456.

[9] B. Hofmann-Wellenhof, H. Lichtenegger, and E. Wasle, *GNSS - Global Navigation Satellite Systems: GPS, GLONASS, Galileo, and more*. Wien: Springer-Verlag, 2007, p. 548.

[10] F. Markley, "Attitude determination using vector observations and the singular value decomposition," *The Journal of the Astronautical Sciences*, vol. 38, no. 3, pp. 245–258, 1988.

[11] R. Roy, "ESPRIT-estimation of signal parameters via rotational invariance techniques," *IEEE Transactions on Acoustics, Speech and Signal Processing*, vol. 37, no. 7, pp. 984–995, 1989.

[12] M. Haardt, "Efficient One-, Two-, and Multidimensional High-Resolution Array Signal Processing," Ph.D. dissertation, Technical University of Munich, 1997.